aEARTHARXIV COVER SHEET

ECMWF SEAS5 Seasonal Precipitation Outlook and Hydrological-Hydrogeological Assessment for the Middle East: August 2026-January 2027

Shaheen Mohammed Saleh Ahmed

Department of Applied Geology, College of Science, University of Kirkuk, Kirkuk, Iraq

Corresponding author: Shaheen Mohammed Saleh Ahmed
Correspondence email: shaheengeolo@gmail.com
ORCID: https://orcid.org/0000-0002-9289-128X
Web of Science ResearcherID: N-6449-2019
SciProfiles ID: 1915829

Preprint declaration

This manuscript is a non-peer-reviewed preprint prepared for submission to EarthArXiv. EarthArXiv moderation is not peer review. The precipitation fields are seasonal ensemble-mean outlook products and are not deterministic weather forecasts, flood warnings, inundation predictions, or quantified groundwater-recharge forecasts.

Manuscript information

Manuscript type: Preprint / hydroclimatic, hydrological and hydrogeological technical research report
Forecast period analysed: August 2026-January 2027
Forecast initialization: 1 August 2026 | ECMWF System 51 ensemble mean
Primary data source: Copernicus Climate Data Store, Seasonal forecast monthly statistics on single levels
Licence selected for EarthArXiv submission: CC BY 4.0
Journal submission status: This manuscript has not been submitted to a peer-reviewed journal at the time of this EarthArXiv submission.

Data and code availability: The ECMWF source dataset is publicly available through the Copernicus Climate Data Store. The supplied research package contains the raw NetCDF, processed precipitation fields in mm/month, tables, and 2-D/3-D figures used in this report. A permanent repository DOI may be added when the package is deposited in a public repository.

Keywords: ECMWF SEAS5; Middle East; seasonal precipitation; hydrology; hydrogeology; groundwater recharge; Eastern Mediterranean; Zagros; Arabian Peninsula; ensemble forecast.

Prepared for EarthArXiv submission: 16 August 2026

ECMWF SEAS5 Seasonal Precipitation Outlook and Hydrological-Hydrogeological Assessment for the Middle East

Forecast period: August 2026-January 2027

Initialization: 1 August 2026 | ECMWF System 51 ensemble mean

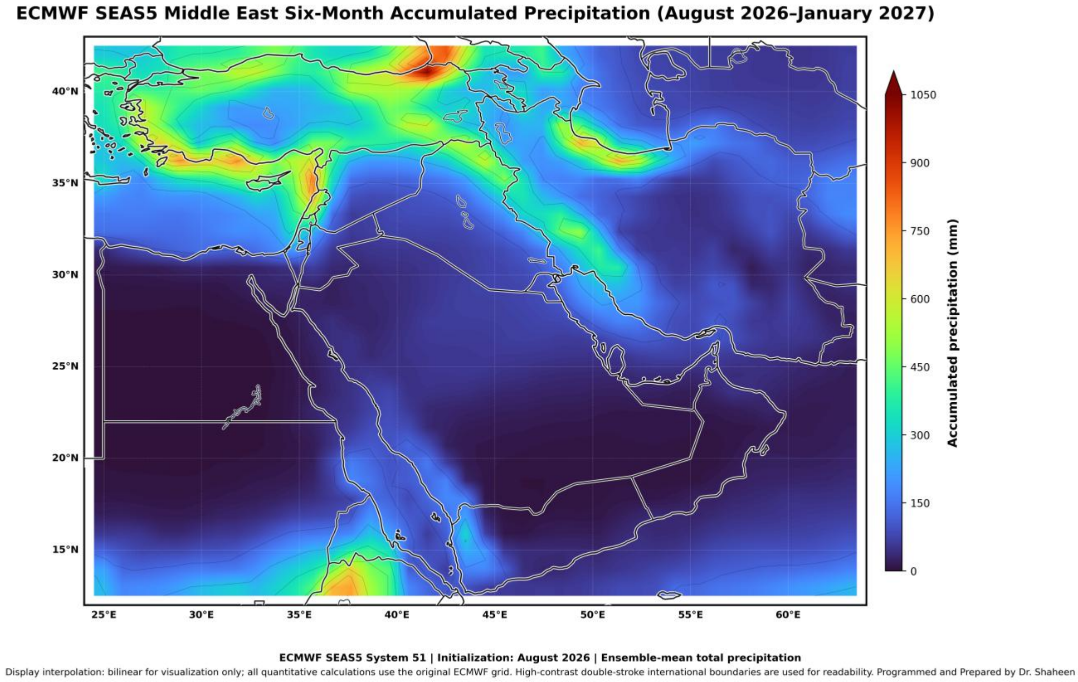

Regional six-month precipitation outlook used as the graphical summary of this preprint.

Source: ECMWF/Copernicus CDS NetCDF values in the supplied analysis package. Bilinear interpolation is display-only; quantitative calculations use the original 1-degree grid.

Programmed and Prepared by Dr. Shaheen

Data processing, hydroclimatic analysis, hydrological and hydrogeological interpretation, cartographic design, and report preparation

August 2026

Abstract

This preprint presents a regional hydrological and hydrogeological interpretation of the ECMWF SEAS5 System 51 ensemble-mean precipitation forecast initialized on 1 August 2026 for the Middle East and adjacent portions of the analysis domain. The supplied NetCDF field is time-mean total precipitation rate (tprate; m s^-1), converted to monthly precipitation depth (mm/month) using the actual number of days in each valid month. Six lead months were analysed, corresponding to August 2026 through January 2027, on the original 1-degree by 1-degree analytical grid. The derived products include monthly precipitation maps, six-month accumulation, October 2026-January 2027 accumulation, peak monthly precipitation, coefficient of variation, representative-city statistics, and three-dimensional visualizations. The strongest six-month accumulation in the grid is 1035.51 mm at 41.5 degrees N, 41.5 degrees E in the eastern Black Sea/northeastern Turkey sector, while the October-January maximum is 830.26 mm at the same grid cell. The largest single-month grid value, 434.62 mm/month at 12.5 degrees N, 37.5 degrees E, lies on the southern fringe of the rectangular domain in the Ethiopian Highlands and is therefore treated separately from the core Middle East interpretation. Among the sampled cities, Erbil has the largest six-month total (581.29 mm), followed by Beirut (510.55 mm) and Istanbul (433.34 mm), whereas Abu Dhabi has the smallest sampled total (38.96 mm). The forecast evolves from predominantly summer-dry conditions across much of the Middle East in August-September toward stronger autumn-winter precipitation across the Eastern Mediterranean, Anatolia, northern Iraq, the Zagros belt, and parts of western and northern Iran. Hydrologically, these patterns indicate where seasonal catchment wetting and runoff loading are greatest, but they do not resolve storm intensity, discharge, or inundation. Hydrogeologically, higher precipitation may enhance recharge opportunity in fractured, karstic, mountain-front, and alluvial aquifers, but precipitation cannot be equated directly with recharge because evapotranspiration, soil storage, runoff, lithology, depth to groundwater, and antecedent moisture control the partitioning of water. The results are therefore presented as an absolute seasonal precipitation outlook rather than an anomaly or flood-hazard forecast; hindcast-based climatology and skill assessment are required before statements of above-normal or below-normal precipitation are made.

Keywords: ECMWF SEAS5; Middle East; seasonal precipitation; hydrology; hydrogeology; groundwater recharge; Eastern Mediterranean; Zagros; Arabian Peninsula; ensemble mean.

Interpretive status

All numerical precipitation values in this report are extracted from the supplied ECMWF analysis package. Bilinear interpolation in the 2-D maps is used only to improve visual presentation; every numerical result is calculated on the original forecast grid. The dataset contains absolute ensemble-mean precipitation totals, not model-climatology anomalies. Accordingly, this report does not classify any area as wetter or drier than normal and does not present flood probability, inundation depth, or groundwater recharge volume.

Contents

1. Introduction and objectives

Seasonal forecasts are designed to describe large-scale shifts in the probability distribution of atmospheric and land-surface conditions over weeks to months, rather than the detailed evolution of individual storms. ECMWF SEAS5 is the fifth-generation ECMWF seasonal forecast system and provides ensemble forecasts and reforecasts through the Copernicus Climate Change Service (C3S). The C3S monthly single-level dataset used here is a global 1-degree by 1-degree product and explicitly characterizes seasonal forecasts as long-range ensemble outlooks with substantial uncertainty compared with short-range weather forecasts (Johnson et al., 2019; C3S, 2026).

The Middle East is an especially demanding region for precipitation interpretation because strong climatic gradients coexist with complex topography, marine influences, desert interiors, and multiple circulation regimes. Winter rainfall over much of the northern Middle East is influenced by Mediterranean and mid-latitude systems, whereas summer rainfall is strongly restricted over most of Arabia but remains important near the southern fringe and southwestern Arabian highlands. Regional modelling studies also show that precipitation representation is sensitive to model resolution and physical parameterization, emphasizing the need to interpret coarse seasonal products at regional rather than local scales (Almazroui et al., 2012; Taraphdar et al., 2021; Charabi & Al-Hatrushi, 2010).

From a water-resources perspective, the same precipitation signal can have very different consequences. In steep or poorly infiltrating catchments it may increase rapid runoff and river response, while in permeable alluvial, fractured, and karstic settings it may contribute to groundwater recharge. In arid aquifer systems, however, recharge is often episodic and small relative to precipitation, and many major groundwater reserves contain a large fossil component accumulated under past wetter climates. Consequently, an academically defensible interpretation must separate precipitation, runoff, recharge opportunity, actual recharge, and long-term groundwater storage change (Scanlon et al., 2002; Scanlon et al., 2006; Rausch & Dirks, 2024).

The objectives of this report are to: (i) document the spatial and temporal structure of the August 2026-January 2027 SEAS5 ensemble-mean precipitation forecast; (ii) quantify forecast totals at representative Middle Eastern city grid cells; (iii) identify the main seasonal precipitation corridors and their evolution from late summer into winter; (iv) interpret hydrological implications for catchment wetting, runoff, and seasonal water availability; (v) discuss hydrogeological implications for recharge opportunity and aquifer response; and (vi) define the additional observations and modelling required for anomaly assessment, flood forecasting, and quantitative groundwater recharge estimation.

2. Study domain and regional hydroclimatic-hydrogeological setting

The rectangular analysis domain spans 24-64 degrees E and 12-43 degrees N. It therefore encompasses Turkey, the Levant, Iraq, Iran, the Arabian Peninsula and Gulf states, and adjacent portions of the eastern Mediterranean, Red Sea, Caspian region, northeastern Africa, and the Horn of Africa. Because the domain is rectangular, its southernmost cells at approximately 12-15 degrees N include areas outside conventional geographic definitions of the Middle East. These fringe cells are retained because they are part of the supplied forecast domain, but they are explicitly separated when regional maxima are interpreted.

The hydroclimatic structure is strongly seasonal. Large parts of the Arabian Peninsula have a wet season concentrated between late autumn and spring and a pronounced summer dry season. Observational climatology for Saudi Arabia shows a broad wet-season/dry-season contrast and especially low rainfall over the Rub al Khali, whereas rainfall belts are stronger to the north and near the southern edge of Arabia (Almazroui et al., 2012). Over the broader Middle East, winter precipitation is often associated with frontal and synoptic systems, while regional topography - including Anatolian mountains, the Zagros, the Levant ranges, and the Hajar Mountains - modifies precipitation spatially (Taraphdar et al., 2021; Charabi & Al-Hatrushi, 2010).

Hydrogeologically, the study domain contains a wide spectrum of aquifer types: karstified carbonate and fractured-bedrock systems in Turkey, the Levant, northern Iraq and the Zagros; intermontane and alluvial basin aquifers in Iraq and Iran; and regionally extensive sandstone and carbonate aquifers on the Arabian Platform. The Upper Mega Aquifer System of the Arabian Platform includes the Wasia-Biyadh sandstone and karstified Umm Er Radhuma and Dammam limestone aquifers; much of the stored groundwater is fossil and modern recharge is limited and spatially concentrated (Rausch & Dirks, 2024). At the same time, regional GRACE-based evidence indicates widespread groundwater-storage stress across the Euro-Mediterranean and Arabian Peninsula, with particularly strong historical declines reported for Iraq and Syria during 2003-2020 (Xanke & Liesch, 2022).

3. Data and analytical methods

3.1 ECMWF seasonal forecast dataset

The supplied research package contains the original ECMWF/Copernicus seasonal monthly single-level NetCDF and a processed analysis-ready NetCDF. The forecast was initialized on 1 August 2026 using ECMWF System 51 and the ensemble mean of total precipitation. The source variable is tprate with units of m s^-1. C3S documents this dataset as monthly gridded seasonal forecast statistics on a global regular 1-degree by 1-degree latitude-longitude grid, with total precipitation expressed as a rate (C3S, 2026).

Table 1. Correct ECMWF lead-month mapping for the August 2026 initialization.

Forecast lead	Valid month
1	August 2026
2	September 2026
3	October 2026
4	November 2026
5	December 2026
6	January 2027

3.2 Conversion from precipitation rate to monthly depth

The time-mean precipitation rate was converted to a monthly depth using Pm = Rp x 1000 x 86,400 x D, where Pm is monthly precipitation in millimetres, Rp is the ECMWF precipitation rate in metres per second, 1000 converts metres to millimetres, 86,400 is the number of seconds per day, and D is the actual number of days in the corresponding valid month. This conversion was applied separately to all six lead months.

3.3 Derived regional metrics

The processed NetCDF includes monthly precipitation, six-month accumulated precipitation (August 2026-January 2027), October 2026-January 2027 accumulation, ASO, SON, OND and NDJ seasonal-window totals, peak monthly precipitation, temporal coefficient of variation, precipitation concentration, and maximum month-to-month increase. The present report focuses on the metrics directly represented in the supplied final figures and city table: monthly totals, six-month accumulation, October-January accumulation, peak monthly precipitation, and month-to-month variability.

3.4 Representative-city extraction

Forecast values for 24 representative cities were extracted from the nearest original ECMWF grid cell. Because the grid spacing is 1 degree, these values characterize regional model cells rather than urban rain gauges or city-scale forecasts. Grid-centre coordinates are reported in Appendix A so that the spatial meaning of each value remains traceable.

3.5 Cartographic visualization

The 2-D maps use bilinear interpolation for display only, together with energetic continuous colour scales and high-contrast international boundaries. Bilinear rendering provides a visually continuous surface but does not create additional meteorological information. All numerical calculations and tabulated values retain the original ECMWF grid. The 3-D figures likewise use vertical height to represent precipitation magnitude, not topographic elevation.

3.6 Interpretation constraints

The current package contains absolute ensemble-mean forecast precipitation, not hindcast-relative anomalies or calibrated probabilities. It is therefore scientifically inappropriate to describe a location as above normal, below normal, anomalously wet, anomalously dry, or more likely than climatology solely from these fields. Such statements require the corresponding System 51 hindcast climatology, lead-specific bias assessment, ensemble spread, and forecast verification. Likewise, monthly precipitation cannot resolve storm intensity, duration, convective organization, river discharge, flood extent, or actual groundwater recharge.

Figure 1. Monthly ECMWF SEAS5 precipitation evolution

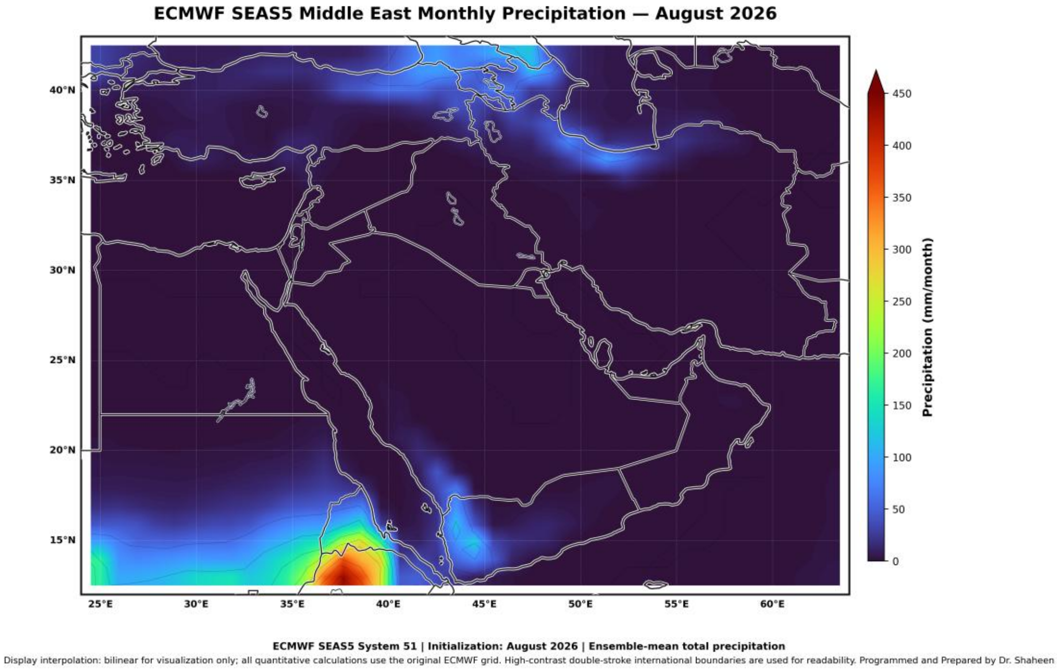

Figure 1a. August 2026 ensemble-mean monthly precipitation.

Source: supplied ECMWF/Copernicus CDS analysis package. Bilinear interpolation is display-only; quantitative values use the original grid.

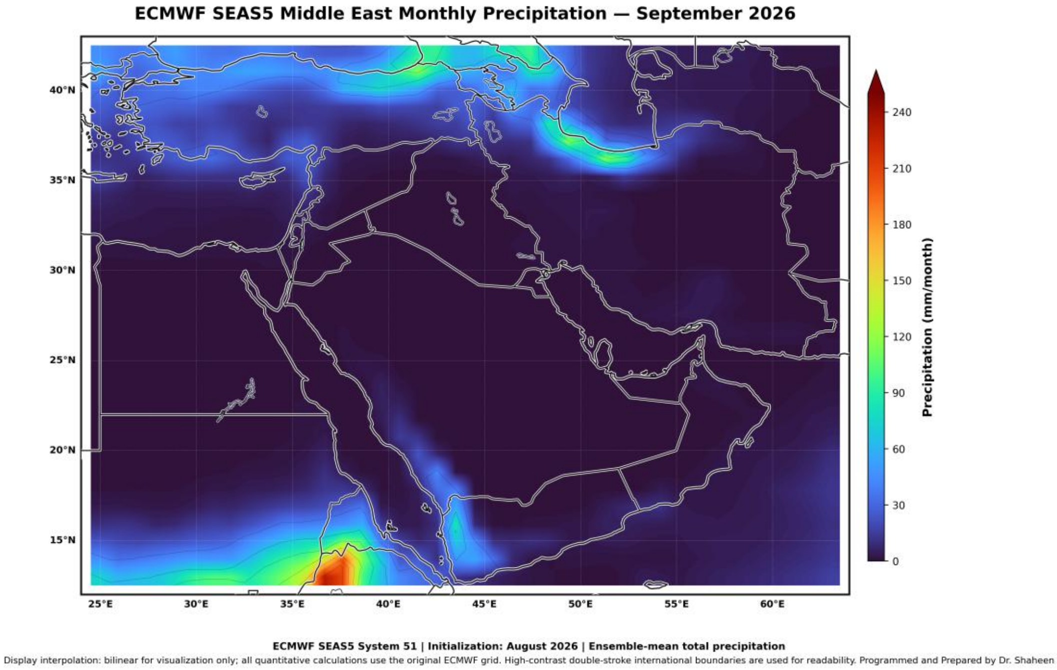

Figure 1b. September 2026 ensemble-mean monthly precipitation.

Source: supplied ECMWF/Copernicus CDS analysis package. Bilinear interpolation is display-only; quantitative values use the original grid.

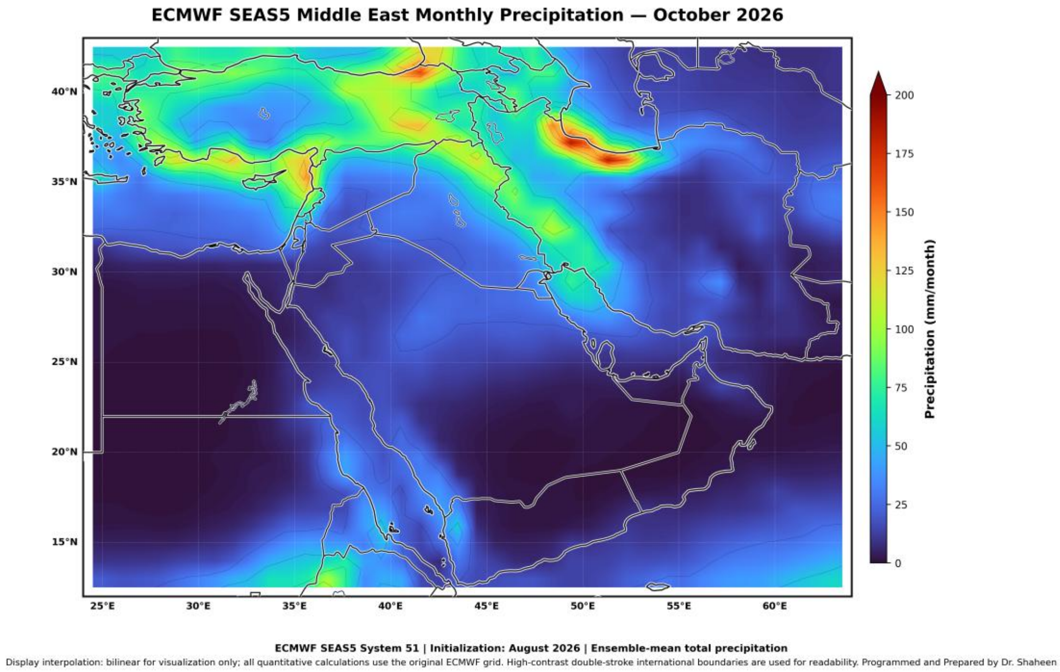

Figure 1c. October 2026 ensemble-mean monthly precipitation.

Source: supplied ECMWF/Copernicus CDS analysis package. Bilinear interpolation is display-only; quantitative values use the original grid.

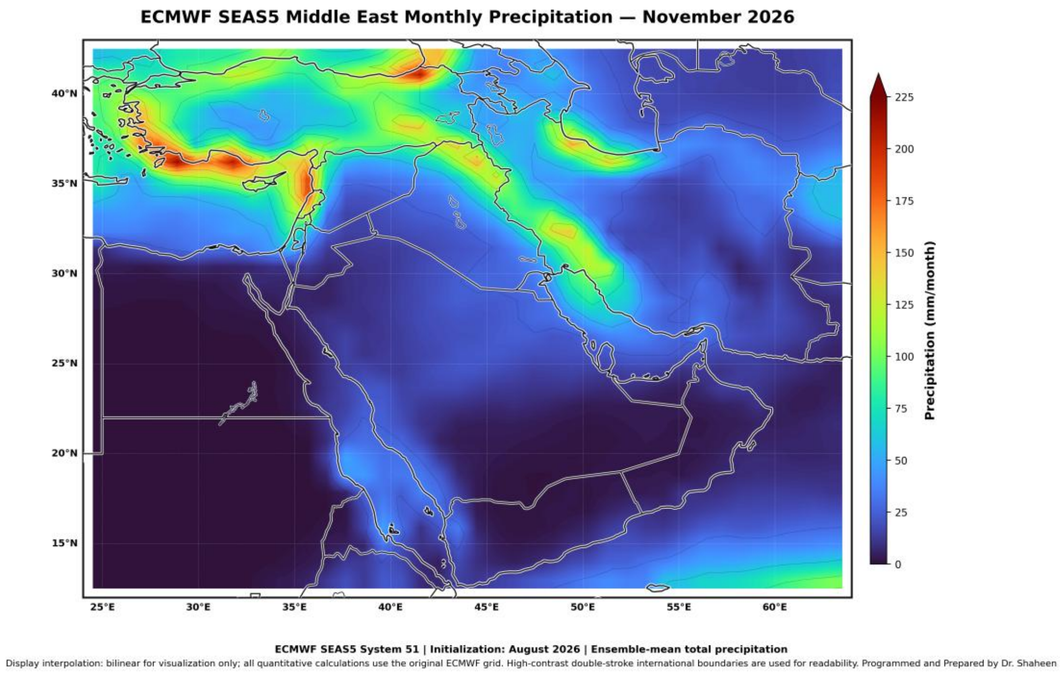

Figure 1d. November 2026 ensemble-mean monthly precipitation.

Source: supplied ECMWF/Copernicus CDS analysis package. Bilinear interpolation is display-only; quantitative values use the original grid.

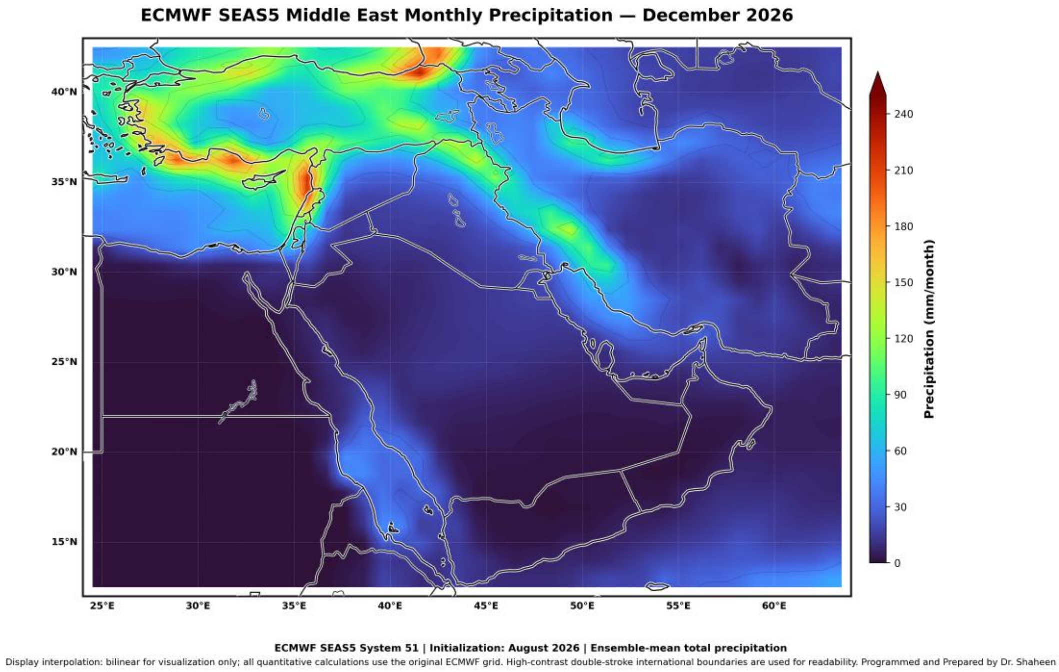

Figure 1e. December 2026 ensemble-mean monthly precipitation.

Source: supplied ECMWF/Copernicus CDS analysis package. Bilinear interpolation is display-only; quantitative values use the original grid.

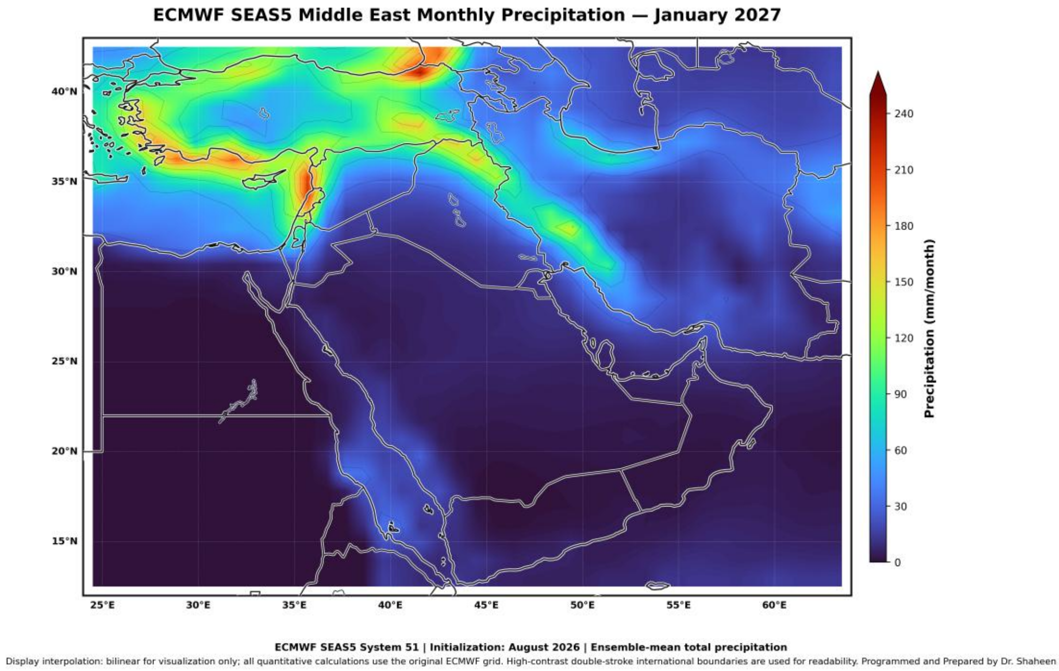

Figure 1f. January 2027 ensemble-mean monthly precipitation.

Source: supplied ECMWF/Copernicus CDS analysis package. Bilinear interpolation is display-only; quantitative values use the original grid.

4. Results

4.1 Seasonal evolution from August 2026 to January 2027

The six monthly maps show a pronounced seasonal reorganization of precipitation. In August and September, most of Iraq, Syria, Jordan, the interior Arabian Peninsula and much of Iran remain at the low end of the forecast range, while higher precipitation is concentrated along parts of northern Turkey/Black Sea influence and the southern fringe of the domain. From October onward, the precipitation field expands and intensifies across the Eastern Mediterranean, Anatolia, northern Iraq, the Zagros belt, and parts of western and northern Iran. November through January form the principal wet-season sequence for much of this northern and western part of the domain, consistent with the broad regional climatological transition toward winter precipitation described in previous Middle East studies (Almazroui et al., 2012; Taraphdar et al., 2021).

The city series quantify this transition. Erbil increases from 2.69 mm in August and 4.36 mm in September to 120.02 mm in October, 152.35 mm in November, 138.35 mm in December, and 163.53 mm in January. Kirkuk shows an even sharper dry-to-wet-season contrast, from less than 1 mm in each of August and September to 84.81-97.50 mm/month in October-November. Beirut similarly increases from 1.40 mm in August and 6.09 mm in September to 65.54 mm in October and 166.76 mm in January. In contrast, Sana'a has its largest monthly value in August (42.09 mm) and declines thereafter, reflecting a different seasonal regime on the southern Arabian highlands.

4.2 Domain-wide maxima

Table 2. Principal precipitation maxima extracted from the supplied processed NetCDF.

Metric	Value (mm)	Lat (N)	Lon (E)	Location
Six-month accumulation (Aug 2026-Jan 2027)	1035.51	41.50	41.50	Eastern Black Sea / northeastern Turkey sector
Oct 2026-Jan 2027 accumulation	830.26	41.50	41.50	Eastern Black Sea / northeastern Turkey sector
Peak single-month value in six-lead domain	434.62	12.50	37.50	Southern fringe / Ethiopian Highlands sector

The highest six-month accumulation is 1035.51 mm at 41.5 degrees N, 41.5 degrees E, and the highest October-January accumulation is 830.26 mm at the same grid cell. This position lies in the eastern Black Sea/northeastern Turkey sector, where maritime moisture and strong orographic control produce a coherent regional precipitation maximum in the supplied forecast. The peak single-month value of 434.62 mm/month occurs at 12.5 degrees N, 37.5 degrees E on the southernmost fringe of the domain, within the Ethiopian Highlands sector. Because this fringe lies outside the core Middle East, it should not be presented as the Middle East precipitation maximum without that geographic qualification.

4.3 Representative-city totals and seasonal timing

Table 3. Representative-city precipitation metrics from the nearest original ECMWF grid cell.

City	Aug-Jan (mm)	Oct-Jan (mm)	Peak month	Peak (mm)	CV (%)
Istanbul	433.34	378.76	December 2026	100.89	46.94
Ankara	220.96	204.24	January 2027	58.14	57.84
Diyarbakir	343.58	338.50	January 2027	98.20	68.69
Aleppo	245.13	240.51	January 2027	73.67	69.67
Beirut	510.55	503.06	January 2027	166.76	76.73
Erbil	581.29	574.25	January 2027	163.53	69.50
Kirkuk	349.93	348.92	November 2026	97.50	70.80
Baghdad	140.64	140.34	October 2026	46.26	76.13
Tabriz	250.96	198.92	October 2026	64.39	32.68
Tehran	143.88	132.36	October 2026	38.76	55.96
Ahvaz	236.64	234.69	November 2026	77.36	75.13
Riyadh	44.42	43.84	November 2026	16.94	79.81
Jeddah	92.25	87.51	December 2026	26.04	63.34
Abu Dhabi	38.96	38.61	November 2026	13.75	78.44
Muscat	43.14	41.90	November 2026	13.48	70.03
Sana'a	72.24	21.72	August 2026	42.09	112.38

Among all 24 sampled cities, Erbil has the largest six-month total (581.29 mm), followed by Beirut (510.55 mm) and Istanbul (433.34 mm). Abu Dhabi has the smallest sampled six-month total (38.96 mm). The wet-season concentration is especially evident when August-September are removed: Erbil retains 574.25 mm during October-January, Beirut 503.06 mm, Istanbul 378.76 mm, Kirkuk 348.92 mm, and Diyarbakir 338.50 mm. These values describe model-cell precipitation loading and should not be treated as local station forecasts.

Peak-month timing varies across the region. January is the wettest forecast month at Erbil, Beirut, Diyarbakir, Aleppo, Damascus, Ankara and Amman. November is the peak month at Kirkuk, Ahvaz and several Gulf cities. October is the peak at Baghdad, Basra, Tabriz, Tehran and Kuwait City. Istanbul peaks in December, while Sana'a peaks in August. This geographic diversity demonstrates why a single Middle East-wide wettest month would be misleading.

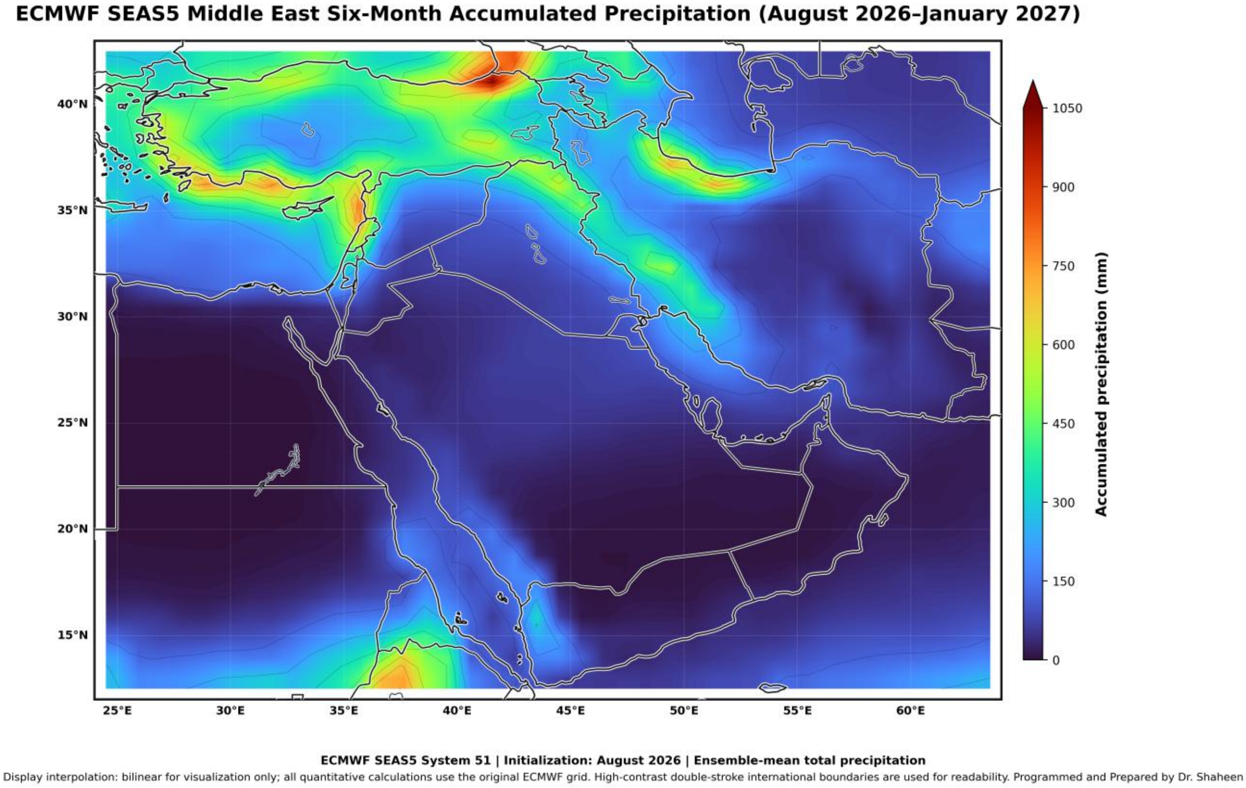

Figure 2. Six-month accumulated ECMWF SEAS5 precipitation for August 2026-January 2027.

The strongest accumulated signal occurs in the eastern Black Sea/northeastern Turkey sector, with secondary high values across the Eastern Mediterranean, northern Iraq/Zagros and adjacent high-relief regions. Values are absolute forecast totals, not anomalies.

Figure 2 integrates the full six-month period and therefore combines two distinct seasonal regimes: late-summer rainfall at the southern fringe and autumn-winter rainfall across the northern Middle East. For water-resources interpretation, the map is most useful as a cumulative atmospheric water-input layer. It does not indicate how much of the precipitation becomes runoff, evapotranspiration, soil-water storage, snow storage, or groundwater recharge.

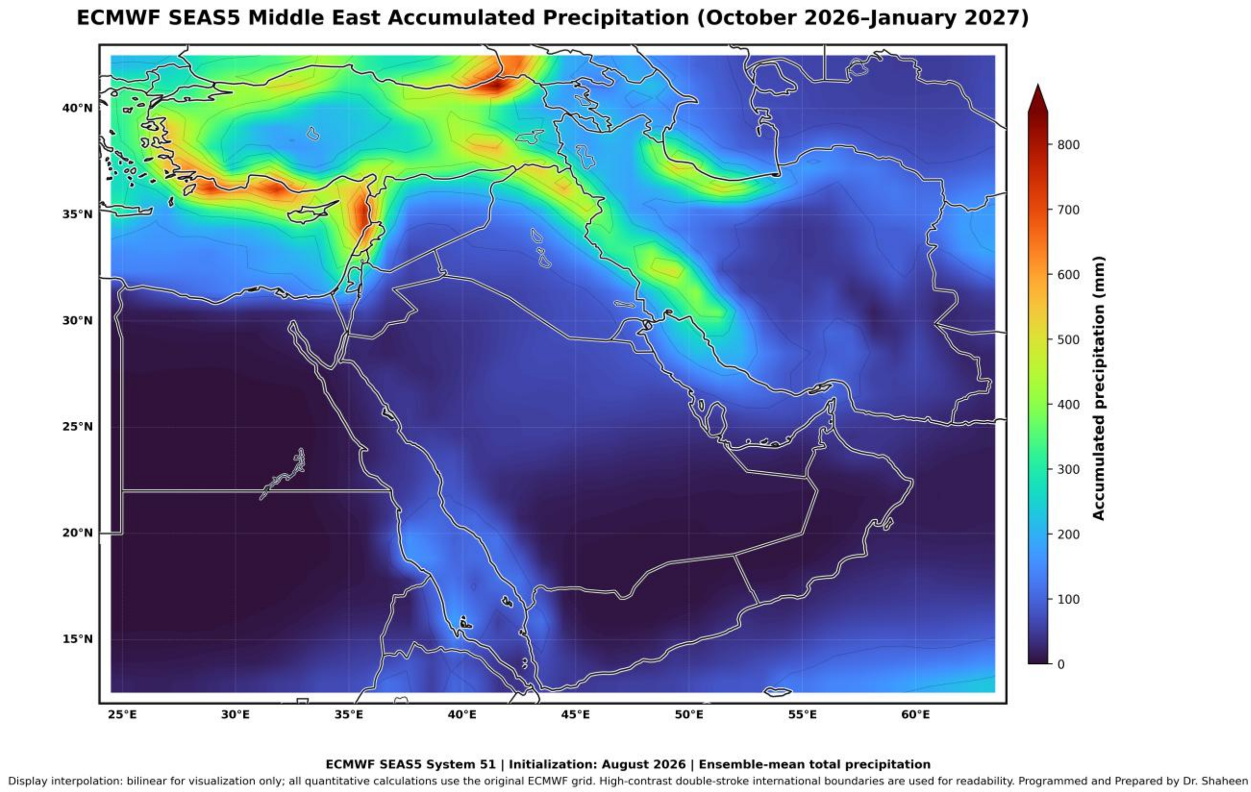

Figure 3. Accumulated ECMWF SEAS5 precipitation for October 2026-January 2027.

This four-month window isolates the principal autumn-winter precipitation season over much of the northern Middle East.

The October-January accumulation removes the strong August-September contribution at the southern fringe and more clearly emphasizes the Eastern Mediterranean-Anatolia-Zagros precipitation corridor. This is also the window most relevant to winter groundwater-recharge opportunity in northern Iraq, the Levant and parts of Iran, although recharge itself remains unquantified.

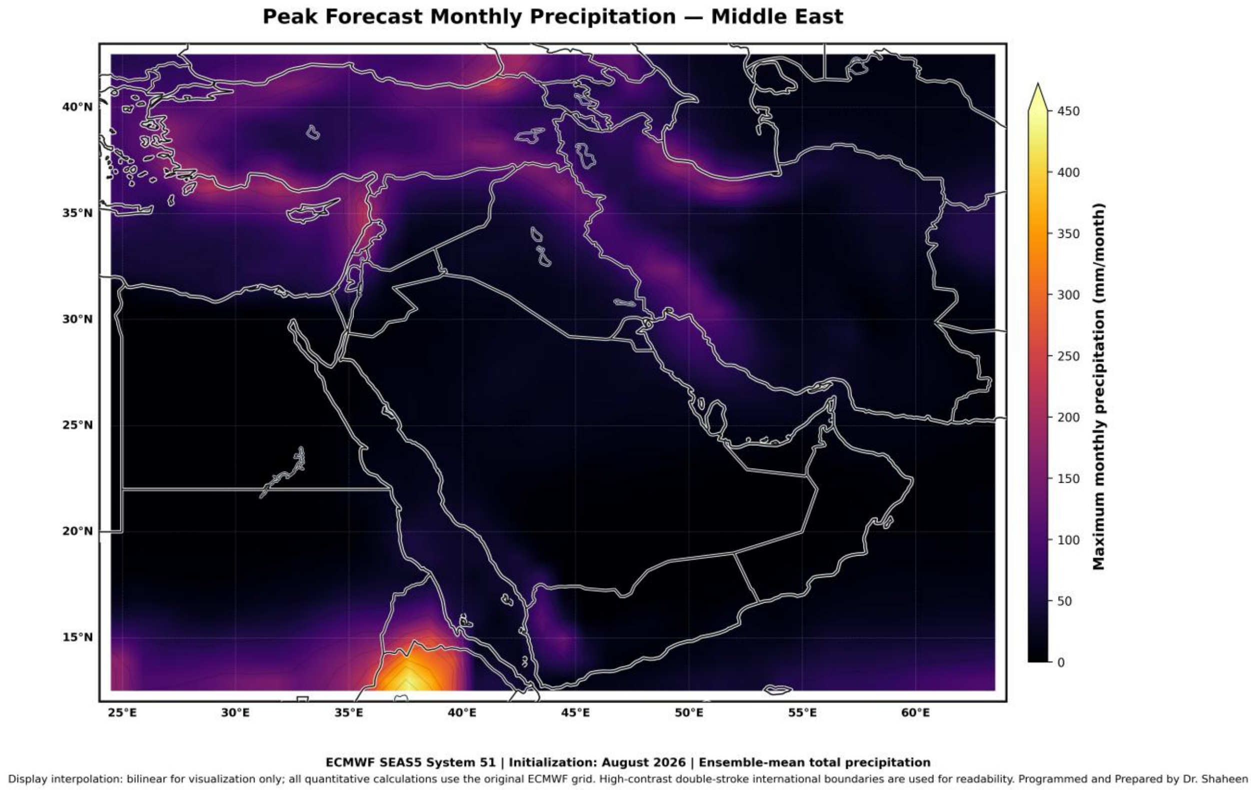

Figure 4. Maximum forecast monthly precipitation across the six lead months.

The map displays the maximum monthly total attained at each grid cell. It does not represent sub-daily storm intensity or peak discharge.

Peak monthly precipitation is a useful indicator of the strongest monthly-scale atmospheric loading, but it cannot diagnose flash-flood intensity. A monthly total can be produced by many moderate storms or a small number of intense events. Flash-flood generation instead depends strongly on storm duration and intensity, catchment morphology, antecedent wetness, drainage connectivity and channel capacity (Borga et al., 2014; Norbiato et al., 2008).

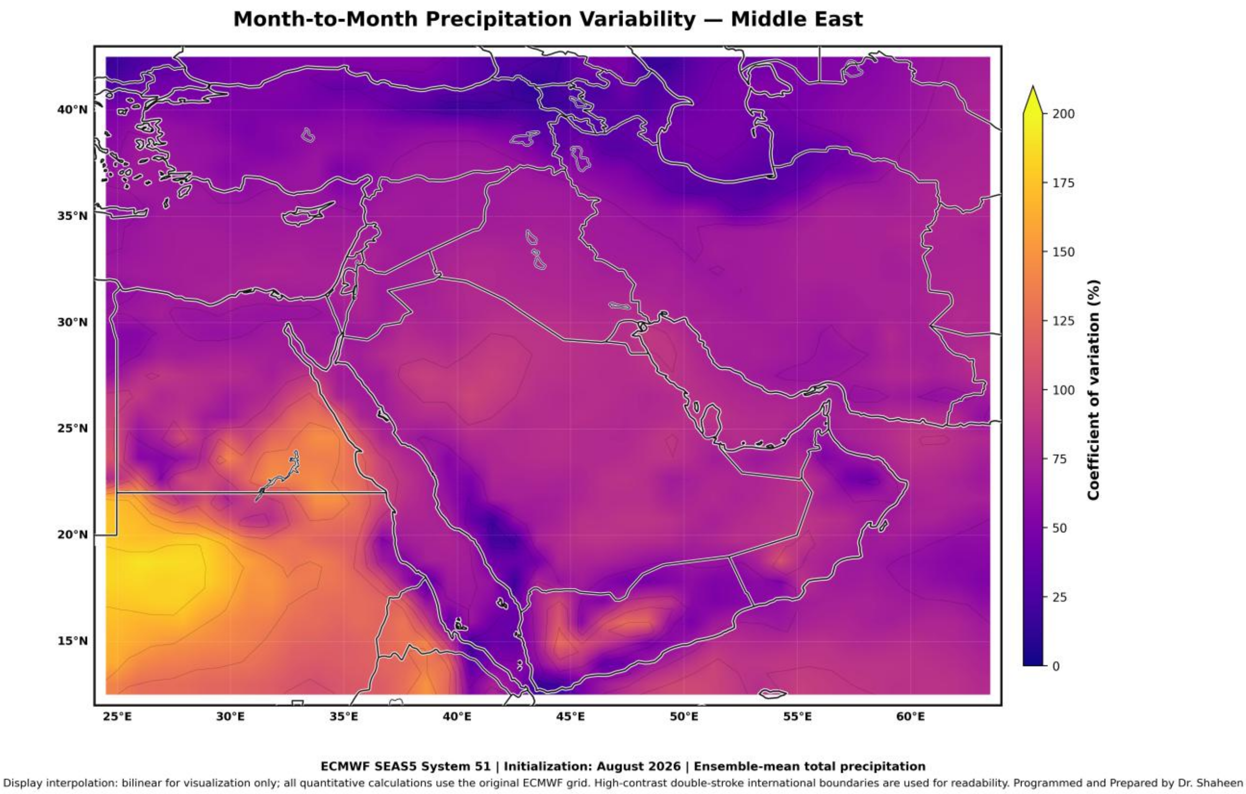

Figure 5. Month-to-month coefficient of variation of forecast precipitation for August 2026-January 2027.

Higher CV indicates a more uneven temporal distribution relative to the local six-month mean; it does not by itself imply a larger precipitation total.

Temporal variability provides information complementary to accumulated precipitation. Very dry summer months followed by wetter autumn-winter months create high coefficients of variation at several arid and transitional sites. For example, Sana'a has the largest sampled CV (112.38%) because its August contribution dominates the series, while Doha, Manama, Kuwait City and Basra also have high CV values because small late-summer totals are followed by episodic autumn-winter precipitation. Istanbul has a lower CV (46.94%) than many arid sites because precipitation is distributed more evenly across the six forecast months.

4.4 Three-dimensional visualizations

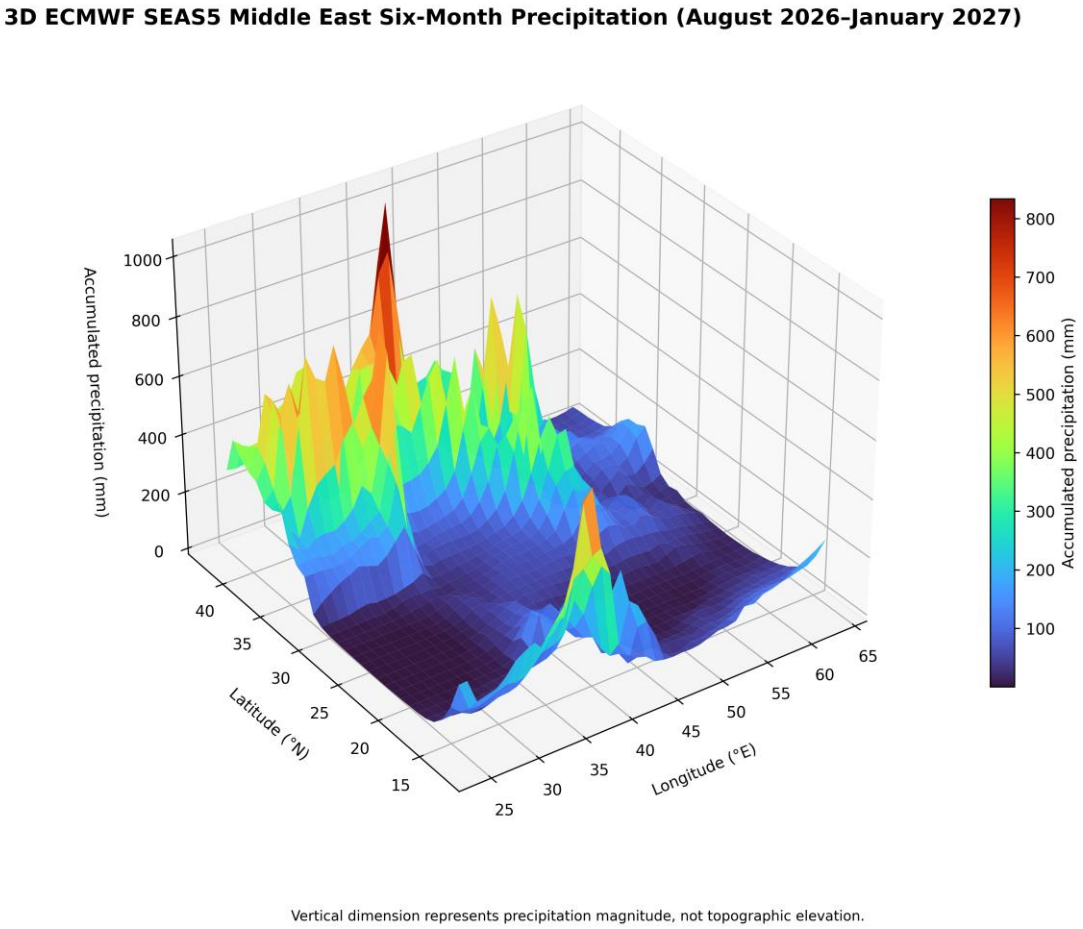

Figure 6. Three-dimensional representation of six-month accumulated precipitation.

Vertical height and colour represent precipitation magnitude; the surface is not topography and does not add resolution beyond the original forecast grid.

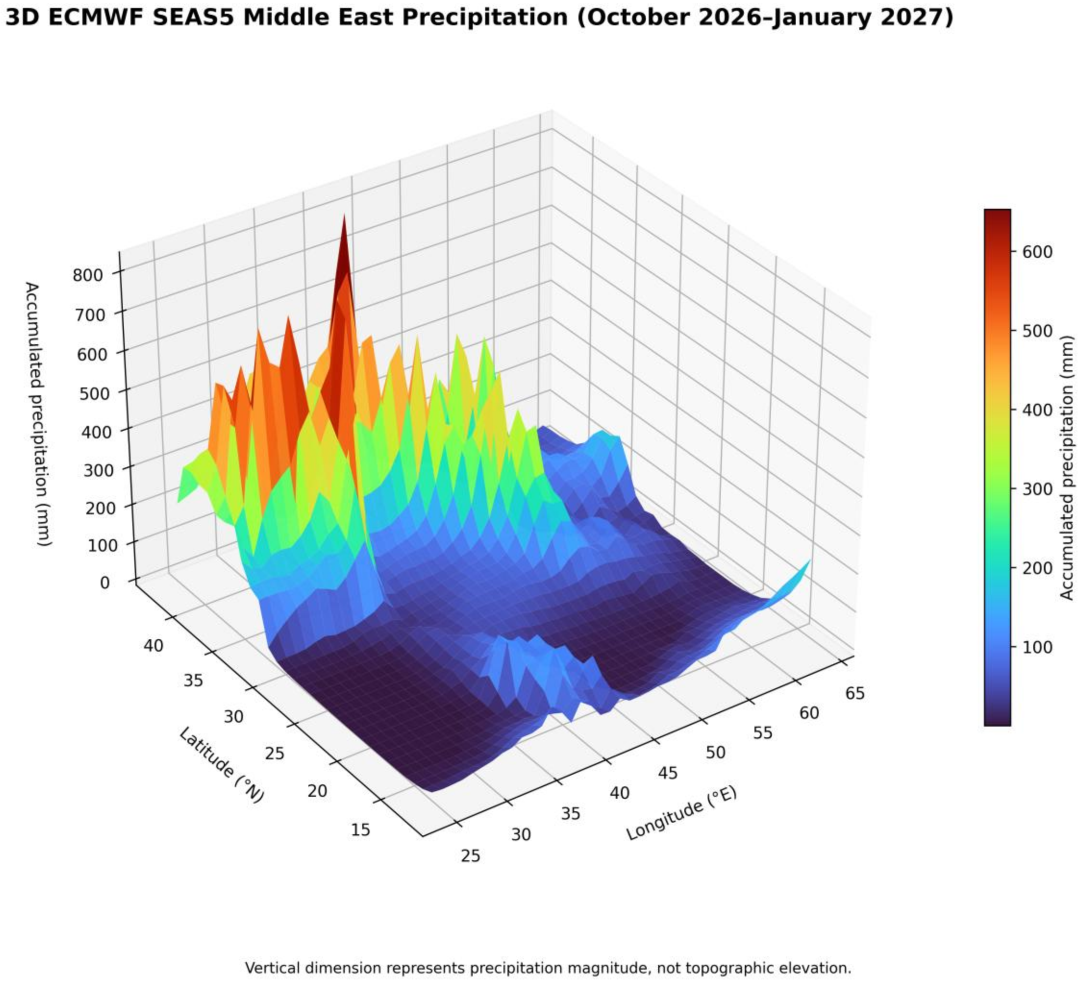

Figure 7. Three-dimensional representation of October 2026-January 2027 accumulated precipitation.

The visualization highlights the steep regional gradient between humid northern/eastern Mediterranean sectors and the arid Arabian interior.

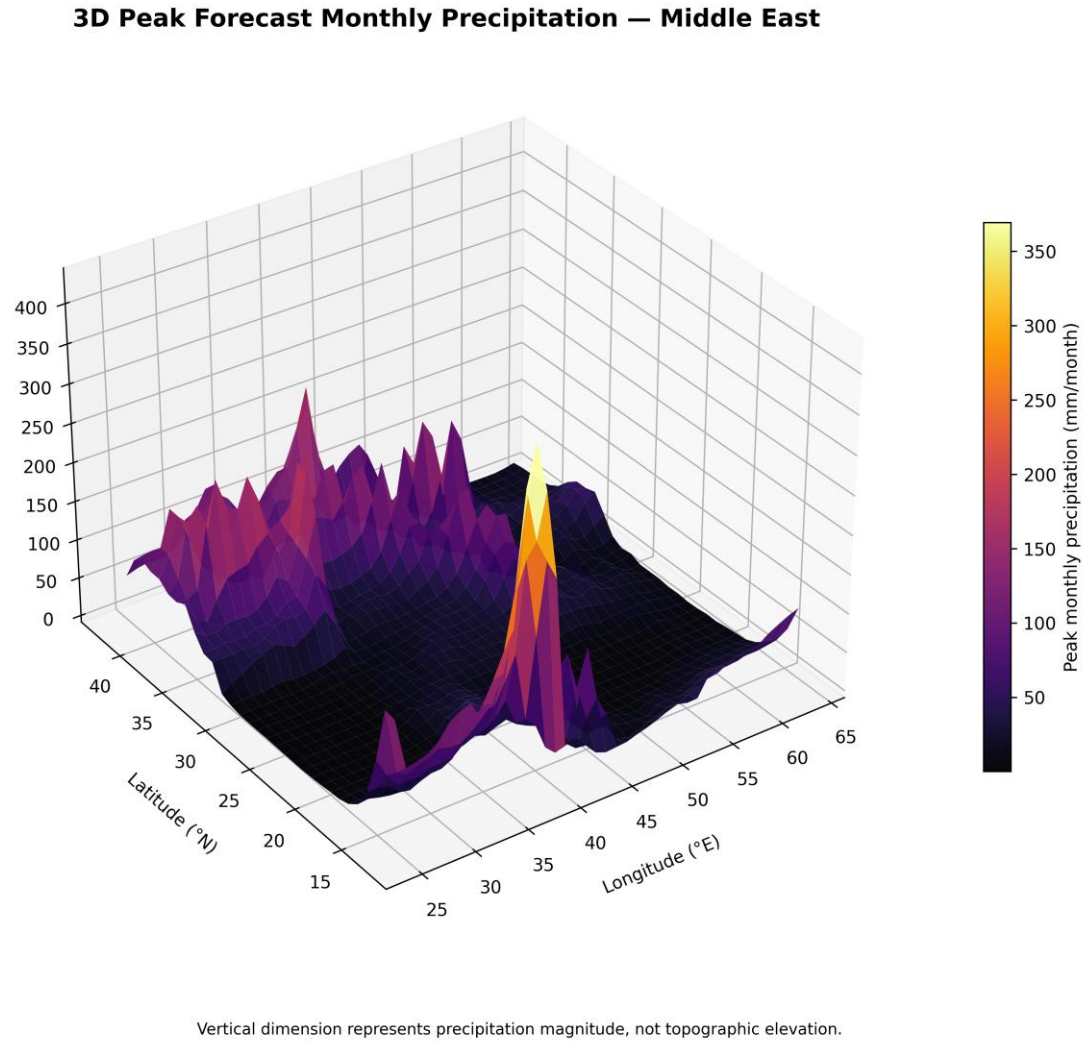

Figure 8. Three-dimensional representation of the maximum monthly precipitation attained during the six-lead forecast.
Vertical height represents forecast precipitation magnitude only, not terrain elevation, discharge, flood depth, or probability.

5. Hydrological interpretation

5.1 Eastern Black Sea and Anatolia

The strongest six-month and October-January grid maxima occur near 41.5 degrees N, 41.5 degrees E in the eastern Black Sea/northeastern Turkey sector. The persistence of high accumulated precipitation in this area suggests sustained seasonal catchment wetting and potentially elevated runoff generation relative to drier interior sectors of the domain. Because the map resolution is 1 degree, the forecast cannot resolve individual mountain basins, snow-rain partitioning, local orographic gradients, or reservoir inflows. Nevertheless, the spatially coherent maximum is hydrologically meaningful at the regional scale and supports closer monitoring of basin-scale precipitation, soil moisture, snow conditions and river response as winter approaches.

Istanbul also shows a comparatively wet six-month sequence (433.34 mm), with monthly totals exceeding 89 mm from October through January and a December peak of 100.89 mm. Ankara is substantially drier (220.96 mm), illustrating the contrast between maritime/northern and continental interior settings. Diyarbakir records 343.58 mm, concentrated strongly from October onward, consistent with its position near the northern Mesopotamian and Anatolian transition.

5.2 Eastern Mediterranean and Levant

Beirut has one of the largest sampled city totals (510.55 mm) and the largest sampled city peak month (166.76 mm in January). Its October-January total is 503.06 mm, indicating that almost the entire six-month accumulation occurs during the autumn-winter season. Aleppo, Damascus and Amman show smaller totals but the same broad winterward increase. The forecast therefore depicts a strong maritime-coastal precipitation gradient into the Levant interior. Such a gradient can have substantial hydrological consequences because short, steep coastal and mountain catchments respond differently from interior plateau basins.

These absolute totals should not be interpreted as a forecast of flood occurrence. Mediterranean catchment response depends on event sequencing, rainfall intensity, soil saturation, slope, land cover, channel geometry and antecedent conditions. As the forecast horizon shortens, this seasonal information should be progressively replaced or complemented by sub-seasonal, medium-range and local observational products.

5.3 Iraq, the Zagros belt and western Iran

The supplied forecast continues the strong north-south hydroclimatic gradient previously identified in the Iraq-only analysis. Erbil records 581.29 mm across August-January and 574.25 mm during October-January, while Kirkuk records 349.93 mm and Baghdad 140.64 mm. Basra is lower still at 114.24 mm. The sharp seasonal transition in Erbil and Kirkuk indicates that catchment wetness and runoff efficiency may rise substantially after October if observed weather evolves in the same direction as the seasonal ensemble mean.

Across Iran, Tabriz has 250.96 mm, Tehran 143.88 mm and Ahvaz 236.64 mm. Their wettest forecast months differ: October at Tabriz and Tehran, November at Ahvaz. The maps also show enhanced accumulation along parts of western and northern Iran relative to the central and southeastern interior. This pattern is compatible with strong topographic and synoptic controls but should not be interpreted as a recharge forecast. Iran has experienced substantial long-term groundwater-recharge decline and depletion, and a single wet seasonal forecast cannot be assumed to reverse that structural water-resource imbalance (Noori et al., 2023).

5.4 Arabian Peninsula and Gulf

The Arabian interior remains comparatively dry in the supplied ensemble mean. Riyadh accumulates 44.42 mm, Abu Dhabi 38.96 mm, Muscat 43.14 mm, Doha 50.78 mm and Dubai 65.05 mm across the six months. Jeddah is higher at 92.25 mm because of its western Arabian setting. These low seasonal totals do not imply absence of pluvial or flash-flood potential. In arid environments, short-duration intense storms over dry, crusted, urbanized or steep catchments can generate damaging runoff even when seasonal rainfall totals are small. Monthly seasonal data cannot resolve such event-scale behaviour.

The temporal pattern is also regionally informative. Several Gulf cities peak in November, while Jeddah peaks in December. Oman remains relatively low at the representative Muscat grid cell, but northern Oman winter rainfall is known to depend on episodic large-scale circulation and Mediterranean-linked troughs (Charabi & Al-Hatrushi, 2010). Consequently, a coarse monthly ensemble mean should be interpreted as background seasonal loading rather than a substitute for storm-scale forecasts.

5.5 Southern fringe and southwestern Arabian seasonal contrast

The largest single-month value in the full rectangular grid occurs at 12.5 degrees N, 37.5 degrees E in August (434.62 mm/month), on the Ethiopian Highlands fringe of the domain. This location is outside the core geographic Middle East and is strongly influenced by a different summer rainfall regime. Sana'a provides a related but smaller southern-Arabian example: 42.09 mm is forecast in August, falling to 3.65 mm by January. These results demonstrate why the regional domain should be interpreted as a set of hydroclimatic subregions rather than as a single homogeneous seasonal system.

6. Hydrogeological interpretation

6.1 Precipitation is not groundwater recharge

Groundwater recharge is the fraction of water that crosses the water table after precipitation has been partitioned among interception, evapotranspiration, runoff, soil-water storage, preferential flow and unsaturated-zone storage. It cannot be calculated from monthly precipitation alone. Robust recharge estimation normally requires multiple independent methods such as water-table fluctuation, environmental tracers, chloride mass balance, soil-water balance, lysimetry, baseflow analysis or calibrated numerical modelling (Scanlon et al., 2002; Healy & Cook, 2002). In semiarid and arid regions, recharge is often episodic and spatially focused, so long-term recharge/precipitation ratios can vary widely (Scanlon et al., 2006).

6.2 Northern mountain belts, karst and fractured aquifers

The strongest forecast precipitation overlaps broad mountain and foothill belts containing fractured and karstic aquifers in Turkey, the Levant, northern Iraq and the Zagros. In such settings, recharge may be enhanced by high-elevation precipitation, snowmelt where present, fractures, faults, sink features, losing stream reaches, alluvial fans and coarse valley fills. The same structural features that promote focused recharge can also produce rapid hydrological response and high spring discharge. Therefore, seasonal precipitation should be coupled with aquifer lithology, fracture density, karst features, elevation, snow conditions and spring/groundwater monitoring before recharge is quantified.

6.3 Northern Iraq

For the Erbil Basin, stable-isotope evidence indicates that local high-altitude precipitation influenced by the Mediterranean sector is a major recharge source, with recharge areas identified at higher elevations (Mamand & Mawlood, 2024). Independent integrated work in the Sulaymaniyah Basin shows that recharge potential depends jointly on rainfall, geology, lineament density, slope, drainage density, land cover and geophysical constraints (Mohammed et al., 2025). The high Erbil and Kirkuk forecast totals therefore imply increased recharge opportunity if future observed precipitation verifies, but they do not provide a recharge rate or groundwater-level forecast.

6.4 Iran

Iran contains extensive alluvial basin aquifers as well as fractured and carbonate systems, but groundwater availability is strongly affected by intensive abstraction and declining recharge. Noori et al. (2023) documented a significant nationwide decline in estimated groundwater recharge over 2002-2017 and emphasized that anthropogenic water management was the dominant driver, compounded by climatic variability. Accordingly, seasonal precipitation maxima over western or northern Iran should be interpreted as potential short-term recharge forcing superimposed on a longer-term depleted groundwater system, not as evidence of resource recovery.

6.5 Arabian Platform aquifers

The Arabian Peninsula hosts very large regional aquifer systems, including the Upper Mega Aquifer System. Rausch and Dirks (2024) describe its major sandstone and karstified limestone aquifers and note that much of the stored groundwater is fossil, recharged under wetter palaeoclimatic conditions. The comparatively small forecast totals across much of Saudi Arabia and the Gulf therefore reinforce the need to distinguish episodic modern recharge from the much larger volume of palaeogroundwater in storage. Localized modern recharge may occur at outcrops, mountain fronts, wadis and karst zones, but monthly precipitation alone cannot determine its amount or sustainability.

6.6 Regional groundwater-storage context

The forecast period should also be viewed against the broader regional groundwater-storage trajectory. Xanke and Liesch (2022) found widespread groundwater-storage declines across the Euro-Mediterranean region during 2003-2020, including strong negative national trends for Iraq and Syria and substantial losses across the Arabian Peninsula. Groundwater systems can buffer short-term meteorological variability because storage integrates recharge and abstraction over time, but persistent pumping can overwhelm episodic wet-season gains. A single seasonal precipitation forecast should therefore inform monitoring priorities rather than be presented as a groundwater-recovery projection (Taylor et al., 2013).

7. Hydrological hazard and water-resources implications

The maps identify areas of high seasonal meteorological loading, especially the eastern Black Sea/northeastern Turkey sector, the Eastern Mediterranean, northern Iraq, and portions of the Zagros and western/northern Iran. In these regions, successive wet months may increase soil moisture, reservoir inflow, streamflow and groundwater-recharge opportunity. However, seasonal monthly totals are not flood-hazard maps. Flood generation requires interaction between precipitation intensity and duration, basin area and relief, drainage-network efficiency, antecedent soil moisture, snowmelt, channel capacity and exposure (Borga et al., 2014; Norbiato et al., 2008).

Conversely, low seasonal totals over the Arabian interior and Gulf should not be interpreted as "low flood risk". Arid-zone floods are often controlled by rare high-intensity storms, impervious or low-infiltration surfaces, steep wadis, urban drainage limitations and short response times. The correct operational use of the current maps is therefore seasonal preparedness: identify regions where wet-season loading deserves closer hydrological monitoring, then update that assessment with shorter-range precipitation ensembles, radar/gauges, soil moisture, wadi/river observations and catchment models as individual events approach.

Required publication wording
This Middle East report does not contain a validated flood-hazard, flood-risk, inundation, or flash-flood prediction map. If a precipitation-derived screening layer is added later, it should be described as a rainfall-based screening or precipitation-only relative susceptibility product unless terrain, catchment, hydraulic, exposure and validation data are incorporated.

8. Uncertainty and limitations

1. The analysis uses the ensemble mean. Ensemble averaging can smooth individual-member extremes and does not show the full forecast distribution or ensemble spread.
2. The analytical resolution is 1 degree by 1 degree. This is appropriate for broad regional interpretation but too coarse for individual wadis, mountain valleys, urban districts, recharge zones or small catchments.
3. Bilinear interpolation is used only for map display. It creates a smoother visual surface but does not create new forecast information; numerical analysis remains on the original grid.
4. Monthly totals do not resolve rainfall intensity, storm duration, convective structure, hourly accumulation, snow-rain partitioning, or event sequencing.
5. The present results are absolute ensemble-mean precipitation totals. No System 51 hindcast climatology, anomaly field, percentile, tercile probability or lead-specific skill score is included in the supplied package.
6. Therefore, the report does not claim that any region is above normal or below normal, and it does not quantify forecast confidence relative to climatology.
7. Representative-city values are nearest-grid values, not station observations or city-scale predictions.
8. The rectangular domain includes southern fringe areas outside conventional definitions of the Middle East; the Ethiopian Highlands grid maximum is explicitly identified as such.
9. The forecast has not been bias-corrected against national gauge networks in this report.
10. Hydrological interpretations do not include DEM-derived runoff routing, soil moisture, river stage, reservoir operations or hydraulic capacity.
11. Hydrogeological interpretations identify plausible recharge opportunity only. They do not estimate groundwater recharge, storage change, spring discharge or water-table rise.
12. Long-range seasonal predictability is inherently variable by region, variable and lead time; precipitation is especially uncertain at local scales (Johnson et al., 2019; C3S, 2026).

9. Recommended next-stage modelling and verification

1. Retrieve the matching ECMWF System 51 hindcasts for the same initialization month and lead times, and compute a model-consistent precipitation climatology.
2. Produce absolute anomalies, percentage anomalies, percentile ranks and tercile probabilities relative to the hindcast distribution rather than inferring anomaly from raw totals.
3. Evaluate hindcast skill over the Middle East using appropriate probabilistic and deterministic verification metrics and stratify by subregion and lead time.
4. Examine individual ensemble members and ensemble spread to characterize uncertainty and the possibility of high-end precipitation outcomes hidden by the ensemble mean.
5. Bias-correct or benchmark monthly totals against quality-controlled national gauges and suitable gridded observational/reanalysis datasets where available.
6. Add forecast surface runoff, soil moisture and snow variables where relevant, and integrate high-resolution DEM, drainage, basin boundaries and land cover for hydrological response analysis.
7. For flash-flood applications, use sub-daily or daily precipitation ensembles, antecedent soil moisture and basin-specific rainfall-runoff models rather than monthly seasonal totals.
8. For groundwater applications, combine precipitation with geology, aquifer properties, vadose-zone thickness, water-table observations, spring hydrographs, stable isotopes, chloride or other tracers, and water-balance modelling.
9. Treat the Arabian fossil-aquifer systems separately from more rapidly responding mountain and alluvial aquifers because modern recharge processes and sustainable yields differ fundamentally.
10. Update the seasonal assessment monthly and progressively replace long-range guidance with extended-range, medium-range and local observations as the forecast horizon shortens.

10. Conclusions

i. The supplied ECMWF SEAS5 System 51 ensemble mean shows a strong spatial and seasonal precipitation gradient across the Middle East from August 2026 to January 2027.

ii. The highest six-month accumulation in the analysis grid is 1035.51 mm at 41.5 degrees N, 41.5 degrees E in the eastern Black Sea/northeastern Turkey sector; the October-January maximum is 830.26 mm at the same grid cell.

iii. The largest single-month value, 434.62 mm/month at 12.5 degrees N, 37.5 degrees E, lies on the southern Ethiopian Highlands fringe of the rectangular domain and should not be reported as a core Middle East maximum without qualification.

iv. Among the 24 representative sampled cities, Erbil has the largest six-month total (581.29 mm), followed by Beirut (510.55 mm) and Istanbul (433.34 mm); Abu Dhabi has the smallest sampled total (38.96 mm).

v. The forecast transitions from widespread late-summer dryness across much of the northern Arabian and Mesopotamian region toward stronger October-January precipitation across the Eastern Mediterranean, Anatolia, northern Iraq, the Zagros and parts of western/northern Iran.

vi. The regional hydrological significance is greatest where high seasonal accumulation combines with steep catchments and progressive wetting, but monthly seasonal totals cannot predict flood occurrence, discharge or inundation.

vii. Higher forecast precipitation may enhance groundwater-recharge opportunity in karstic, fractured, mountain-front and alluvial aquifers, but actual recharge cannot be calculated from precipitation alone.

viii. In Iran and much of the Arabian Peninsula, the seasonal precipitation outlook must be interpreted against documented long-term groundwater stress and, in parts of Arabia, the dominance of fossil groundwater storage.

ix. Because the supplied product contains absolute ensemble-mean totals rather than climatological anomalies, no above-normal or below-normal classification is made in this report.

x. The highest-priority methodological extension is to integrate System 51 hindcasts, ensemble spread and forecast skill with basin-scale hydrological data and groundwater observations.

Data, programming, and authorship statement

ECMWF/Copernicus seasonal forecast data were downloaded in NetCDF format and processed into monthly precipitation depths in millimetres. The supplied research package includes the original data file, processed NetCDF, representative-city CSV, summary JSON, and high-resolution 2-D/3-D figures. Conversion, derived analysis, cartographic design, hydrological and hydrogeological interpretation, and preparation of this report were programmed and prepared by Dr. Shaheen. Quantitative results in this manuscript were taken from the supplied package rather than estimated from the map colours.

Data and code availability

The ECMWF seasonal forecast source data are available from the Copernicus Climate Data Store dataset "Seasonal forecast monthly statistics on single levels" (DOI: 10.24381/cds.68dd14c3). This study used ECMWF System 51 ensemble-mean total precipitation initialized on 1 August 2026. The accompanying research package contains the raw and processed NetCDF products, tabulated city values, summary metrics and derived figures used here. A permanent Zenodo or institutional repository DOI can be inserted after public deposition of the package.

Author contribution and responsibility statement

Shaheen Mohammed Saleh Ahmed conceived the regional assessment, prepared the Python processing and visualization workflow, assembled the ECMWF data products, interpreted the hydrological and hydrogeological results, and wrote the manuscript. The author is responsible for maintaining the distinction between seasonal precipitation guidance, hydrological response, groundwater recharge opportunity, and validated hazard or recharge estimates.

References

Reference verification note: Bibliographic metadata and DOI links were checked on 16 August 2026 against publisher pages or official Copernicus/ECMWF resources. References are included only where they support the data description, regional hydroclimatic interpretation, hydrological process discussion, or hydrogeological context.

Almazroui, M., Islam, M. N., Jones, P. D., Athar, H., & Rahman, M. A. (2012). Recent climate change in the Arabian Peninsula: Seasonal rainfall and temperature climatology of Saudi Arabia for 1979-2009. Atmospheric Research, 111, 29-45. https://doi.org/10.1016/j.atmosres.2012.02.013

Borga, M., Stoffel, M., Marchi, L., Marra, F., & Jakob, M. (2014). Hydrogeomorphic response to extreme rainfall in headwater systems: Flash floods and debris flows. Journal of Hydrology, 518, 194-205. https://doi.org/10.1016/j.jhydrol.2014.05.022

Charabi, Y., & Al-Hatrushi, S. (2010). Synoptic aspects of winter rainfall variability in Oman. Atmospheric Research, 95(4), 470-486. https://doi.org/10.1016/j.atmosres.2009.11.009

Copernicus Climate Change Service (C3S). (2026). Seasonal forecast monthly statistics on single levels. Climate Data Store. https://doi.org/10.24381/cds.68dd14c3

Healy, R. W., & Cook, P. G. (2002). Using groundwater levels to estimate recharge. Hydrogeology Journal, 10, 91-109. https://doi.org/10.1007/s10040-001-0178-0

Johnson, S. J., Stockdale, T. N., Ferranti, L., Balmaseda, M. A., Molteni, F., Magnusson, L., Tietsche, S., Decremer, D., Weisheimer, A., Balsamo, G., Keeley, S. P. E., Mogensen, K., Zuo, H., & Monge-Sanz, B. M. (2019). SEAS5: The new ECMWF seasonal forecast system. Geoscientific Model Development, 12, 1087-1117. https://doi.org/10.5194/gmd-12-1087-2019

Mamand, B. S., & Mawlood, D. K. (2024). Identifying sources of groundwater and recharge zone using stable environmental isotopes in the Erbil basin-northern Iraq. Kuwait Journal of Science, 51(1), 100128. https://doi.org/10.1016/j.kjs.2023.09.002

Mohammed, S. H., Mohammed, M. A. A., Karim, H. A., et al. (2025). Integrating geospatial, hydrogeological, and geophysical data to identify groundwater recharge potential zones in the Sulaymaniyah basin, NE of Iraq. Scientific Reports, 15, 9920. https://doi.org/10.1038/s41598-025-94603-z

Noori, R., Maghrebi, M., Jessen, S., et al. (2023). Decline in Iran's groundwater recharge. Nature Communications, 14, 6674. https://doi.org/10.1038/s41467-023-42411-2

Norbiato, D., Borga, M., Degli Esposti, S., Gaume, E., & Anquetin, S. (2008). Flash flood warning based on rainfall thresholds and soil moisture conditions: An assessment for gauged and ungauged basins. Journal of Hydrology, 362(3-4), 274-290. https://doi.org/10.1016/j.jhydrol.2008.08.023

Rausch, R., & Dirks, H. (2024). A hydrogeological overview of the Upper Mega Aquifer System on the Arabian Platform. Hydrogeology Journal, 32, 621-634. https://doi.org/10.1007/s10040-023-02760-0

Scanlon, B. R., Healy, R. W., & Cook, P. G. (2002). Choosing appropriate techniques for quantifying groundwater recharge. Hydrogeology Journal, 10(1), 18-39. https://doi.org/10.1007/s10040-001-0176-2

Scanlon, B. R., Keese, K. E., Flint, A. L., Flint, L. E., Gaye, C. B., Edmunds, W. M., & Simmers, I. (2006). Global synthesis of groundwater recharge in semiarid and arid regions. Hydrological Processes, 20, 3335-3370. https://doi.org/10.1002/hyp.6335

Taraphdar, S., Pauluis, O. M., Xue, L., Liu, C., Rasmussen, R., Ajayamohan, R. S., et al. (2021). WRF gray-zone simulations of precipitation over the Middle-East and the UAE: Impacts of physical parameterizations and resolution. Journal of Geophysical Research: Atmospheres, 126, e2021JD034648. https://doi.org/10.1029/2021JD034648

Taylor, R. G., Scanlon, B., Doell, P., et al. (2013). Ground water and climate change. Nature Climate Change, 3, 322-329. https://doi.org/10.1038/nclimate1744

Xanke, J., & Liesch, T. (2022). Quantification and possible causes of declining groundwater resources in the Euro-Mediterranean region from 2003 to 2020. Hydrogeology Journal, 30, 379-400. https://doi.org/10.1007/s10040-021-02448-3

Appendix A. Full representative-city forecast table

Table A1 reports all 24 representative grid cells contained in the supplied city CSV. Values are nearest-grid ECMWF ensemble-mean totals and are not gauge observations. The full monthly columns are retained to support traceability and independent checking of the regional interpretation.

Table A1. ECMWF SEAS5 monthly precipitation at representative Middle East grid cells (mm/month).

City	Lat	Lon	Aug	Sep	Oct	Nov	Dec	Jan	Aug-Jan
Istanbul	41.50	28.50	7.72	46.87	91.67	89.85	100.89	96.35	433.34
Ankara	39.50	32.50	2.92	13.81	38.19	53.32	54.59	58.14	220.96
Diyarbakir	37.50	40.50	0.47	4.60	79.68	84.89	75.73	98.20	343.58
Aleppo	36.50	37.50	1.29	3.32	48.13	53.33	65.38	73.67	245.13
Damascus	33.50	36.50	0.31	1.60	23.70	31.93	34.53	45.27	137.35
Beirut	33.50	35.50	1.40	6.09	65.54	124.89	145.87	166.76	510.55
Amman	31.50	35.50	0.35	1.17	16.64	30.16	37.20	43.77	129.30
Erbil	36.50	44.50	2.69	4.36	120.02	152.35	138.35	163.53	581.29
Kirkuk	35.50	44.50	0.19	0.81	84.81	97.50	77.90	88.71	349.93
Baghdad	33.50	44.50	0.00	0.30	46.26	40.19	27.17	26.72	140.64
Basra	30.50	47.50	0.08	0.85	40.22	37.19	20.07	15.83	114.24
Tabriz	38.50	46.50	26.27	25.78	64.39	52.30	42.06	40.17	250.96
Tehran	35.50	51.50	6.12	5.40	38.76	36.34	27.79	29.47	143.88
Ahvaz	31.50	48.50	0.16	1.79	67.95	77.36	45.57	43.81	236.64
Kuwait City	29.50	47.50	0.04	0.57	32.60	31.48	17.97	11.58	94.23
Riyadh	24.50	46.50	0.00	0.59	10.03	16.94	10.47	6.40	44.42
Jeddah	21.50	39.50	0.70	4.04	19.31	25.01	26.04	17.15	92.25
Medina	24.50	39.50	1.01	2.23	17.24	13.58	9.65	5.79	49.50
Doha	25.50	51.50	0.00	0.32	10.83	22.25	9.96	7.41	50.78
Manama	26.50	50.50	0.00	0.17	20.19	27.82	13.66	8.77	70.61
Abu Dhabi	24.50	54.50	0.12	0.23	5.51	13.75	10.64	8.71	38.96
Dubai	25.50	55.50	0.08	0.30	11.50	22.16	18.69	12.32	65.05
Muscat	23.50	58.50	0.43	0.81	11.40	13.48	10.08	6.94	43.14
Sana'a	15.50	44.50	42.09	8.43	7.09	6.36	4.62	3.65	72.24

EarthArXiv submission compliance note

This manuscript includes a dedicated coversheet as page 1, author affiliation and correspondence email, full ORCID URL, and an explicit statement that the manuscript is a non-peer-reviewed preprint prepared for submission to EarthArXiv. If the manuscript is subsequently submitted to a peer-reviewed journal, the journal name should be added to the coversheet statement before resubmission. If the accompanying data/code package receives a permanent DOI, that DOI should also be inserted in the Data and code availability section.